

Surface electronic structure of the $\text{NdB}_6(110)$ clean surface studied by angle-resolved photoemission spectroscopy

Akinori Tanaka, Koji Tamura, Hiroshi Tsunematsu, Kazutoshi Takahashi, Masayuki Hatano, Shoji Suzuki, Shigeru Sato, and Satoru Kunii

Department of Physics, Graduate School of Science, Tohoku University, Aoba-ku, Sendai 980-77, Japan

Ayumi Harasawa, Akio Kimura, and Akito Kakizaki

Synchrotron Radiation Laboratory, Institute for Solid State Physics, University of Tokyo, Minato-ku, Tokyo 106, Japan

(Received 30 January 1997)

An angle-resolved photoemission study of the $\text{NdB}_6(110)$ clean surface has been done in order to investigate in detail the surface electronic structure. From the dependence of the valence-band photoemission spectra on the surface condition and the exciting photon energy, we found additional peaks corresponding to the surface states on the $\text{NdB}_6(110)$ surface. These surface states are located at around 1.8 eV in binding energy. The dispersion relations of these surface states were determined along the $\bar{\Gamma}-\bar{M}$ symmetry line in the surface Brillouin zone and it is found that the energy dispersion for the present surface state is about 250 meV. From the photon energy dependence and the analogy of these observations with previous results for the $\text{LaB}_6(110)$ clean surface, it is concluded that the present surface states have the same specifications as those of the $\text{LaB}_6(110)$ surface and are ascribed to the B $2p$ dangling bonds of the surface B framework.

[S0163-1829(97)08235-0]

I. INTRODUCTION

The surface electronic states of the rare-earth compounds recently have been attracting much interest because they are expected to differ from the bulk electronic states. For example, α -like Ce compounds show a strong change of the $4f$ electronic structure toward a more localized γ -like behavior with increasing the degrees of surface sensitivity for photoemission spectroscopy.^{1,2} The heavy rare-earth metals such as Sm, Eu, Tm, and Yb show the surface valence transitions.³⁻⁵ On the other hand, the surface electronic structure is characterized mainly by the specification of the surface states. Such surface states on the clean surface of semiconductors and elemental metals have been studied fairly well both experimentally and theoretically. Regarding the rare-earth compounds, to our knowledge, surface states on the $\text{LaB}_6(100)$, (110) , (111) ,⁶ and (001) (Ref. 7) clean surface and $\text{CeNi}(010)$ (Ref. 8) clean surface have been observed by angle-resolved photoemission spectroscopy and Ce $4d$ - $4f$ resonant photoemission spectroscopy, respectively. Since almost all previous photoemission studies of the rare-earth compounds have been done against the clean surface prepared by scraping, reports of the existence of the surface state and the difference between the surface and bulk electronic states are very few to date for the rare-earth compounds.

The present NdB_6 , as well as other rare-earth hexaborides, has a simple cubic CsCl crystal structure where a rare-earth atom (Nd atom) is located at the center and eight regular octahedrons consisting of six B atoms are located at the corners surrounding a rare-earth atom (Nd atom). In NdB_6 , the spins align antiferromagnetically in the z direction at $T_N=8.6$ K and the antiferromagnetic phase has a simple tetragonal magnetic structure.⁹ The self-consistent electronic

structures of both paramagnetic and antiferromagnetic phases for NdB_6 using the linearized muffin-tin orbital band method within the local-density approximation (LDA) have been reported.¹⁰ In addition, the energy band calculation has been performed recently by the Korringa-Kohn-Rostoker method based on the LDA and the calculated Fermi surface reproduces the results of de Haas-van Alphen measurements fairly well.¹¹

In this work, we carried out the angle-resolved photoemission study of a single-crystalline $\text{NdB}_6(110)$ clean surface so as to elucidate the surface electronic structure of NdB_6 . The angle-resolved photoemission spectroscopy has been used to determine the specification of the surface states on the clean surface, but, to our knowledge, there is no report of an angle-resolved photoemission study to date that highlights the surface electronic structure of NdB_6 . Since the band calculations of NdB_6 (Refs. 10 and 11) have been reported already and the angle-resolved photoemission study of the LaB_6 clean surface^{6,7} has been carried out already, we pay attention to the single-crystalline $\text{NdB}_6(110)$ clean surface and carry out a comparative angle-resolved photoemission study with LaB_6 . From these results, we discuss the surface states that characterize the surface electronic states on the $\text{NdB}_6(110)$ clean surface.

II. EXPERIMENT

The angle-resolved photoemission measurements were carried out with a ultrahigh vacuum (UHV) photoelectron spectrometer that consists of a hemispherical electron analyzer, a He discharge lamp, an Auger electron spectrometer with a double cylindrical mirror analyzer, and low-energy electron diffraction (LEED) optics. A hemispherical electron analyzer could be rotated around a sample in an UHV chamber. The base pressure of the spectrometer was better than

about 2×10^{-8} Pa. The total energy resolution for the measurement excited by He I resonance radiation ($h\nu = 21.2$ eV) was about 200 meV and the angle resolution was about $\pm 1.5^\circ$.

The additional resonant photoemission measurements using synchrotron radiation were carried out at BL-18A of the Photon Factory, National Laboratory for High Energy Physics (KEK), Tsukuba, Japan. The exciting photon energies used in this experiment were 128 and 120 eV, which corresponded to Nd $4d-4f$ on and off resonance, respectively.¹² We used a CLAM (VG Scientific Co. Ltd.) angle-integrated electron analyzer with an acceptable angle of $\pm 24^\circ$ for these resonant photoemission measurements. The base pressure of the spectrometer was better than about 5×10^{-9} Pa. The total energy resolution in these photon energies was about 250 meV.

The single-crystalline NdB_6 used in our experiment was synthesized by the floating zone method. The thin sample disk with a thickness of about 0.8 mm parallel to the (110) plane was cut from the single-crystal rod. The sample surface was mirror polished by a suspension of carborundum and alumina powder. The crystal structure and the crystal orientation were checked by x-ray-diffraction measurement. The prepared sample was cleaned in organic solution before introducing it to the UHV photoemission spectrometer. Under the ultrahigh vacuum in the photoemission spectrometer, the sample surface was cleaned by repeated cycles of annealing around 900 °C and flashing to around 1200 °C by electron-beam bombardment. The cleanliness and structure of the sample surface were checked by Auger signals and LEED patterns. By the above method, we observed a clear LEED pattern and succeeded in getting the uncontaminated clean surface. Nishitani *et al.*⁶ have reported that the clean surface of single-crystalline $\text{LaB}_6(110)$ prepared by a method similar to our present experiment has shown the surface reconstruction, that is, the $c(2 \times 2)$ structure. However, it is found that the present $\text{NdB}_6(110)$ surface shows a clear (1×1) LEED pattern, indicative of no surface reconstruction.

From the orientation of the LEED pattern, we decided the photoelectron detection plane for the angle-resolved photoemission measurements. All photoemission measurements reported here were recorded at room temperature. The photoemission spectra showed no change in the course of the measurements. The contamination of the sample surface was monitored by the presence of O and C *KLL* Auger signals, which were negligible throughout the measurements. The surfaces were kept clean during the measurements by occasionally repeating the annealing and flashing *in situ* described above. The Fermi level of the sample was determined by comparison with a gold film deposited on the sample surface.

III. RESULTS AND DISCUSSION

Figure 1(a) (bottom) shows the angle-resolved valence-band photoemission spectrum at normal emission measured at room temperature for the single-crystalline $\text{NdB}_6(110)$ clean surface excited by the He I resonance line ($h\nu = 21.2$ eV) and Fig. 1(b) (bottom) shows the derivative Auger electron spectrum corresponding to the valence-band photoemission spectrum shown in Fig. 1(a). As shown in

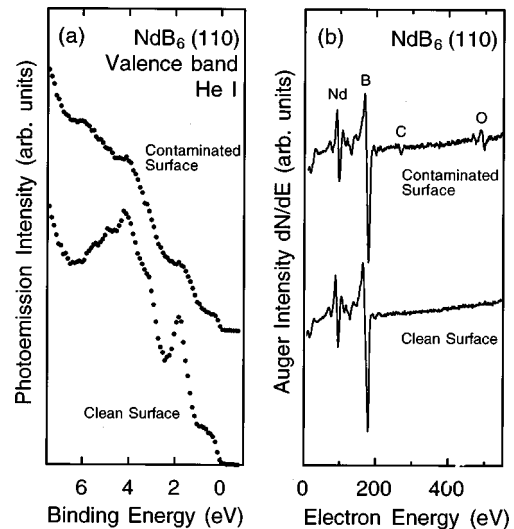


FIG. 1. (a) Angle-resolved valence-band photoemission spectra at normal emission for the clean surface (bottom) and the contaminated surface (top) of single-crystalline $\text{NdB}_6(110)$ measured with He I resonance radiation ($h\nu = 21.2$ eV) at room temperature. (b) Derivative Auger electron spectra of the $\text{NdB}_6(110)$ surface corresponding to the valence-band photoemission spectrum as shown in (a).

Fig. 1(b), the Auger electron spectrum for the present single-crystalline $\text{NdB}_6(110)$ clean surface shows no traces of contamination. This indicates that the present method for preparing the clean surface is effective for the $\text{NdB}_6(110)$ surface. As shown in Fig. 1(a), the valence-band photoemission spectrum of the $\text{NdB}_6(110)$ clean surface shows small structures around 3–5 eV binding energy. From a comparison with the band calculation for NdB_6 ,^{10,11} it is considered that these structures correspond to the B $2s$ and $2p$ derived states. In addition to these B $2s$ and $2p$ derived states, the spectrum shows a sharp peak with higher intensity around 1.8 eV binding energy. In order to check the contamination effect on the surface for this peak, the spectrum after exposure of the $\text{NdB}_6(110)$ clean surface to a worse vacuum is shown in the upper part of Fig. 1(a) and the derivative Auger electron spectrum corresponding to this contaminated surface is shown in the upper part of Fig. 1(b). As shown in Fig. 1(b), the surface after exposure of the clean surface to a worse vacuum is mainly contaminated with oxygen and carbon. The structures around 3–5 eV binding energy in the valence-band spectrum for the thus contaminated surface become much broader and additional intensity appears around 5–6 eV binding energy. This additional intensity around 5–6 eV is due to the oxygen derived states, as is well known. The prominent change by contaminating the surface is the gradual disappearance of the intense peak observed around 1.8 eV binding energy. It is found that this intense sharp peak around 1.8 eV observed for the $\text{NdB}_6(110)$ clean surface depends on the surface condition; this indicates that this peak is related to the $\text{NdB}_6(110)$ surface.

Figure 2 shows the angle-resolved valence-band photoemission spectra at normal emission for the single-crystalline $\text{NdB}_6(110)$ clean surface taken with He I ($h\nu = 21.2$ eV) (bottom) and He II ($h\nu = 40.8$ eV) (top) resonance lines as the exciting light. Each structure observed in the valence-

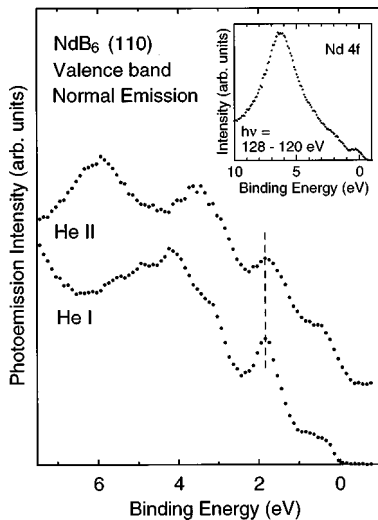


FIG. 2. Angle-resolved valence-band photoemission spectra at normal emission for the single-crystalline $\text{NdB}_6(110)$ clean surface measured with the He I resonance line ($h\nu=21.2$ eV) (bottom) and He II resonance line ($h\nu=40.8$ eV) (top) at room temperature. The inset shows the difference of the photoemission spectrum between the Nd $4d$ - $4f$ on-resonance spectrum taken at $h\nu=128$ eV and the off-resonance spectrum taken by $h\nu=120$ eV at room temperature.

band spectrum with the He II resonance line is slightly broader than that with He I resonance line due to the worse energy resolution. In the inset of Fig. 2, we plot the Nd $4f$ derived spectrum for the single-crystalline $\text{NdB}_6(110)$ clean surface, which is derived by taking the difference between the Nd $4d$ - $4f$ on-resonance spectrum with $h\nu=128$ eV and the off-resonance spectrum with $h\nu=120$ eV.¹² In the valence-band spectrum taken with the He II resonance line, an additional feature at about 6 eV binding energy is observed and is ascribed to the Nd $4f$ states, as is also seen in the Nd $4f$ derived photoemission spectrum shown in the inset of Fig. 2. This is because the relative photoionization cross section of Nd $4f$ electrons to B $2s$ and $2p$ electrons is large at the photon energy of He II resonance line ($h\nu=40.8$ eV) and thus the result clearly appears in the valence-band spectrum. Using this variation of the photoionization cross section of rare-earth $4f$ electrons, rare-earth $4f$ states often have been manifested by the difference between the photoemission spectra measured with the He I and He II resonance lines in many previous photoemission studies. The B $2s$ and $2p$ derived structures around 3–5 eV in the valence-band spectrum taken with the He I resonance line shift to the lower-binding-energy side in the spectrum taken with the He II resonance line. Since the changes of exciting photon energy at normal emission correspond to the change of the corresponding wave vector perpendicular to sample surface, it shows that the B $2s$ and $2p$ derived bands have a energy dispersion along the direction perpendicular to sample surface.

An important point to note is that the sharp structure around 1.8 eV binding energy in the valence-band spectrum with the He I resonance line exhibits no energy shift with changing exciting photon energy, as denoted by the dashed line in Fig. 2. This means that the electronic states corresponding to this sharp structure around 1.8 eV binding energy have no energy dispersion along the direction perpen-

dicular to sample surface and are two-dimensional electronic states. From the comparison between the valence-band spectra for clean and contaminated surfaces, it is found that the sharp intense peak around 1.8 eV depends on the surface condition, as described above. In addition, it is found that this peak exhibits no three-dimensional energy dispersion at present. Furthermore, compared to the band calculation for NdB_6 ,^{10,11} there is no bulk electronic band states around this energy region. Therefore, it is concluded that this sharp structure around 1.8 eV binding energy is ascribed to the surface states on the $\text{NdB}_6(110)$ clean surface. Nishitani *et al.*⁶ reported similar surface states around 1.8 eV binding energy for the $\text{LaB}_6(110)$ clean surface. Furthermore, they found the symmetry of the wave functions of these surface states and thereby concluded that these surface states on the $\text{LaB}_6(110)$ clean surface were ascribed to the dangling bonds of the surface boron framework, which is mainly B $2p$ in character. In the present case of the $\text{NdB}_6(110)$ clean surface, the binding energies of the observed surface states are almost the same as those of the $\text{LaB}_6(110)$ clean surface reported by Nishitani *et al.* In addition, the intensity of the present surface states decreases with increasing photon energy from $h\nu=21.2$ eV (He I resonance line) to 40.8 eV (He II resonance line). This systematic change as a function of the photon energy is due to the photon energy dependence of the photoionization cross section of the constituent atomic orbitals. The photoionization cross section of B $2p$ electrons decreases with increasing photon energy. Therefore, we conclude that the present surface states have the same specifications as those of the $\text{LaB}_6(110)$ surface and may be ascribed to the B $2p$ electrons. Nishitani *et al.*⁶ also reported that the $\text{LaB}_6(110)$ clean surface showed the $c(2\times 2)$ surface reconstruction structure caused by a displacement of the surface La atoms^{6,13} and concluded that these surface states on the $\text{LaB}_6(110)$ clean surface were associated with the occurrence of the $c(2\times 2)$ surface structure. However, it is found that the present surface states are observed on the $\text{NdB}_6(110)$, 1×1 clean surface and have a 1×1 structure. On the other hand, from the result of the Nd $4d$ - $4f$ photoemission spectrum as shown in the inset of Fig. 2, the Nd $4f$ derived spectrum has no prominent peak structure around 1.8 eV binding energy, indicating that the present surface states have no $4f$ character such as the surface states observed on CeNi(010) clean surface.⁸

In order to study the two-dimensional energy dispersions of these surface states on the $\text{NdB}_6(110)$ surface, we measured the angle-resolved photoemission spectra at various photoelectron emission angle in the $(1\bar{1}0)$ plane. This detection plane corresponds to trace of the $\bar{\Gamma}$ - \bar{M} symmetry line in the surface Brillouin zone (SBZ) and the normal emission is associated with the photoemission from the center of SBZ of $\bar{\Gamma}$ symmetry point. Figure 3 shows the angle-resolved photoemission spectra at various detection angles in the (110) plane for the single-crystalline $\text{NdB}_6(110)$ clean surface measured with the He I resonance line ($h\nu=21.2$ eV). The detection angles are with respect to the surface normal direction. As shown in Fig. 3, the overall spectral features observed in the $(1\bar{1}0)$ plane for the present $\text{NdB}_6(110)$ are almost the same as those for $\text{LaB}_6(110)$. This means that the valence-band electronic structure for $\text{NdB}_6(110)$ is almost

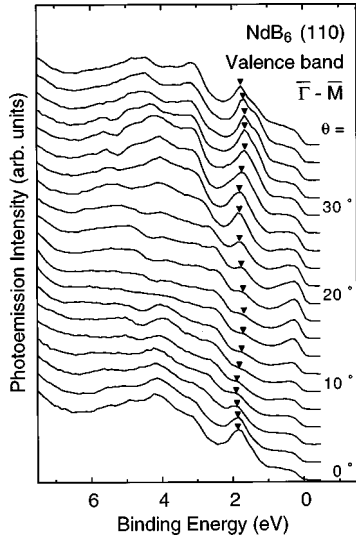


FIG. 3. Angle-resolved valence-band photoemission spectra at various photoelectron emission angles in the $(1\bar{1}0)$ plane for the single-crystalline $\text{NdB}_6(110)$ clean surface measured with the He I resonance line ($h\nu=21.2$ eV) at room temperature. Solid triangles indicate the peaks from the surface states. The emission polar angles with respect to the surface normal are indicated on the right-hand side.

the same as that for $\text{LaB}_6(110)$, and this result is consistent with the similarity of band calculation for NdB_6 (Refs. 10 and 11) and $\text{LaB}_6(110)$.^{14,15} This is because the valence bands of the rare-earth hexaborides consist mainly of B $2s$ and $2p$ electrons. However, it is difficult to discuss the bulk electronic band structures from each observed structure on the angle-resolved photoemission spectra due to the existence of many electronic bands within the valence-band region according with the band calculations and it is beyond the scope of this paper. Hence we will not discuss the bulk band electronic structures in more detail and will discuss below the angle-resolved photoemission spectra from surface states in particular. As shown in Fig. 3, we can see the surface states denoted by solid triangles even changing the photoelectron detection angle up to around $\theta=40^\circ$. The intensities of the surface state peaks decrease and increase once as the photoelectron detection angle increases from the normal emission of $\theta=0^\circ$ up to about $\theta=32^\circ$ and then the intensities decrease again. These changes of the intensities reflect that $\theta=0^\circ$ and about 32° , compared to the binding energies of these surface states, correspond to the center of SBZ ($\bar{\Gamma}$ symmetry points) and the zone boundary of SBZ (\bar{M} symmetry point), respectively. From this result it is found again that the periodicity of the present surface states has a 1×1 structure and is determined by the 1×1 SBZ. Furthermore, it is found that the binding energies of these surface states change as a function of photoelectron emission angle. This means that these surface states have the two-dimensional energy dispersion along the $\bar{\Gamma}$ - \bar{M} symmetry line on SBZ. These energy dispersions are discussed below.

In order to clarify the dispersion relations of these surface states on the $\text{NdB}_6(110)$ clean surface, we plot the binding energies E_B of these surface states versus the wave vector parallel to the sample surface k_{\parallel} along the $\bar{\Gamma}$ - \bar{M} symmetry

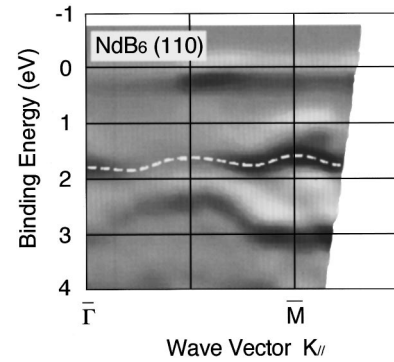


FIG. 4. Energy dispersion relation of the surface states along the $\bar{\Gamma}$ - \bar{M} symmetry line of the surface Brillouin zone for the single-crystalline $\text{NdB}_6(110)$ clean surface. This E_B versus k_{\parallel} diagram is expressed by the gray scale of the secondary derivative of the angle-resolved photoemission spectra. The white dashed line is drawn to guide the eyes for the energy dispersion relation of the surface states.

line in the SBZ in Fig. 4. To derive the wave vector k_{\parallel} from the binding energies and the photoelectron detection angles, we use $\phi=3.16$ eV for the work function of the $\text{NdB}_6(110)$ clean surface, which is experimentally determined from the leading edge of the secondary electrons on the photoemission spectrum. It is found that this work function of $\phi=3.16$ eV for $\text{NdB}_6(110)$ is fairly larger than that of $\phi=2.5$ eV for $\text{LaB}_6(110)$, which is known well as an electron-beam source of high brightness.^{16,17} The E_B versus k_{\parallel} diagram as shown in Fig. 4 is expressed by the following method. The secondary derivative of each angle-resolved photoemission spectrum with respect to E_B is taken at first. After that, each differentiated spectrum is converted to a gray-scale bar and then the gray-scale bars of a set of angle-resolved photoemission spectra are arranged to the corresponding coordinates in the E_B - k_{\parallel} plane, where the abscissa is k_{\parallel} and the ordinate is E_B . In this diagram, the darkness in the bar roughly corresponds to the intensity of the peak. That is, this diagram shows both the energy position and the intensity of each observed electronic state. As shown in Fig. 4, it is recognized that the intensities increase around $\bar{\Gamma}$ and \bar{M} symmetry points as described above. It is clear that the dispersion relation of the surface states is symmetric to the \bar{M} symmetry point of the SBZ, indicating that these surface states have a 1×1 structure. Furthermore, it is clear that the surface states on the $\text{NdB}_6(110)$ surface has an energy dispersion along the $\bar{\Gamma}$ - \bar{M} symmetry line of the SBZ as described above and the dispersion relation of these surface states was definitely determined in the SBZ. This dispersion relation is indicated by the white dashed line in Fig. 4. It is found that the energy dispersion of these surface states is quite small, of the order of about 250 meV. This energy dispersion is almost the same as that along the $\bar{\Gamma}$ - \bar{M}' symmetry line of $\text{LaB}_6(110)$, where the \bar{M}' symmetry point is the zone boundary of the SBZ for the $c(2\times 2)$ reconstructed surface and the direction of $\bar{\Gamma}$ - \bar{M}' symmetry line is the same as that of the present $\bar{\Gamma}$ - \bar{M} symmetry point. It is indicated again that the specification of these surface states on the $\text{NdB}_6(110)$ surface is the same as that on the $\text{LaB}_6(110)$ surface. Namely, these surface states are associated with the

dangling bonds of the surface B framework, which is constructed by strong covalent bonding in regular octahedrons consisting of six B atoms. Since the $c(2 \times 2)$ reconstructed surface on the $\text{LaB}_6(110)$ surface is caused by a displacement of the surface La atoms,¹³ the B framework is not greatly affected by the surface reconstruction of the $c(2 \times 2)$ structure. Therefore, the specifications of the surface states, which are derived from the dangling bonds of the B framework, are also not greatly affected by the surface reconstruction. This may be the reason why the surface states having specifications similar to those of the $\text{LaB}_6(110)$, $c(2 \times 2)$ clean surface are observed on the $\text{NdB}_6(110)$, 1×1 clean surface. These results lead to the speculation that the surface states having the same specifications will also be observed even for other rare-earth hexaborides. According to the analysis of the symmetry of the wave function from the polarization-dependent photoemission study for the $\text{LaB}_6(110)$ surface,⁶ the wave functions of these surface states are mainly made up of B $2p$ orbitals which make an angle of 45° with the (110) surface. Since the dangling bonds of B atoms on the $\text{NdB}_6(110)$ surface are attributed to the present surface state at an incline at 45° to the (110) surface, the wave function may overlap with neighboring wave functions of the surface states fairly small. Therefore, the present small dispersion of about 250 meV for the surface states on the $\text{NdB}_6(110)$ clean surface considered to originate from a quite small overlapping of the wave function of the surface state.

IV. CONCLUSION

We have performed an angle-resolved photoemission study for the single-crystalline $\text{NdB}_6(110)$ clean surface. In the valence-band photoemission spectrum, we observed the additional intense peak around 1.8 eV binding energy. From a comparison of the valence-band spectra for clean and contaminated surfaces and the photon energy dependence, it was found that this additional peak originated from the surface states on the $\text{NdB}_6(110)$ surface. Through detailed angle-resolved photoemission measurements along the $\bar{\Gamma}$ - \bar{M} symmetry line in the surface Brillouin zone, it is found that the energy dispersion of the present surface states is quite small, of the order of about 250 meV. From the photon energy dependence and the analogy of these observations with previous results for the $\text{LaB}_6(110)$ clean surface, the present surface states are considered to have the same specifications as those of the $\text{LaB}_6(110)$ surface and are ascribed to the B $2p$ dangling bonds of the surface B framework.

ACKNOWLEDGMENTS

This work was supported by a Grant-in-Aid for Scientific Research from the Ministry of Education, Science and Culture of Japan. This work was partly performed under the Photon Factory Proposal No. 95G390.

¹C. Laubschat, E. Weschke, C. Holtz, M. Domke, O. Strebel, and G. Kaindl, *Phys. Rev. Lett.* **65**, 1639 (1990).

²E. Weschke, C. Laubschat, T. Simmons, M. Domke, O. Strebel, and G. Kaindl, *Phys. Rev. B* **44**, 8304 (1991).

³G. K. Wertheim and G. Crecelius, *Phys. Rev. Lett.* **40**, 813 (1978).

⁴B. Johansson, *Phys. Rev. B* **19**, 6615 (1979).

⁵C. Laubschat, G. Kaindl, W.-D. Schneider, B. Reihl, and N. Martensson, *Phys. Rev. B* **33**, 6675 (1986).

⁶R. Nishitani, M. Aono, T. Tanaka, S. Kawai, H. Iwasaki, C. Oshima, and S. Nakamura, *Surf. Sci.* **95**, 341 (1980).

⁷M. Aono, T. Tanaka, E. Bannai, C. Ohima, and S. Kawai, *Phys. Rev. B* **16**, 3489 (1977).

⁸T. Kashiwakura, S. Suzuki, T. Okane, S. Sato, T. Kinoshita, A. Kakizaki, T. Ishii, Y. Isikawa, H. Yamagami, and A. Hasegawa, *Phys. Rev. B* **47**, 6885 (1993).

⁹C. M. McCarthy and C. W. Tompson, *J. Phys. Chem. Solids* **41**, 1319 (1980).

¹⁰B. I. Min and Y.-R. Jang, *Phys. Rev. B* **44**, 13 270 (1991).

¹¹Y. Kubo, S. Asano, H. Harima, and A. Yanase, *J. Phys. Soc. Jpn.* **62**, 205 (1993).

¹²A. Tanaka, K. Tamura, K. Takahashi, M. Hatano, T. Okane, S. Suzuki, S. Sato, S. Kunii, A. Harasawa, A. Kimura, and A. Kakizaki, *Physica B* (to be published).

¹³R. Nishitani, M. Aono, T. Tanaka, C. Oshima, S. Kawai, H. Iwasaki, and S. Nakamura, *Surf. Sci.* **93**, 535 (1980).

¹⁴A. Hasegawa and A. Yanase, *J. Phys. F* **7**, 1245 (1977).

¹⁵H. Harima, O. Sakai, T. Kasuya, and A. Yanase, *Solid State Commun.* **66**, 603 (1988).

¹⁶L. W. Swanson and T. Dickinson, *Appl. Phys. Lett.* **28**, 578 (1976).

¹⁷L. W. Swanson and D. R. McNeely, *Surf. Sci.* **83**, 11 (1979).